Chapter 2
Electrochemical Exfoliation Synthesis of Graphene

The synthesis of graphene in both high quality and quantity *via* economic ways is highly desirable and meaningful for practical applications. Here a facile, environmentally-friendly and cost-effective multiple electrochemical exfoliation approach has been developed for the synthesis of high quality graphene flakes with high yield by using graphite rod from spent zinc-carbon/pencil core as carbon source. Various protonic acid (i.e H_2SO_4, H_3PO_4 or $H_2C_2O_4$) aqueous solution were chosen as electrolyte. The unique cell configuration enables multiple exfoliation process to improve both the quality and yield of graphene sheets. After nitrogen doping, the exfoliated graphene flakes process good electrocatalytic activity, stability and toxicity tolerance for alkaline solution-based oxygen reduction reaction.

2.1 Introduction

Since the first fabrication of single-sheet graphene through micromechanical cleavage of bulk graphite was reported [1], numbers of methods have been developed for generating graphene with high quality and low cost. Micromechanical cleavage [1], chemical vapor deposition (CVD) [2, 3] and epitaxial growth [4] produce graphene with high crystal quality but they are impractical for commercial applications due to low production rate and relatively high cost. Chemical exfoliation of graphene based on Brodie, Staudenmaier and Hummers methods, which involves the oxidation of graphite with oxidants and strong acids, and the subsequent chemical or thermal reduction, is advantageous in terms of low cost and controllable solution-processing [5]. However, this method employs some hazardous chemicals (e.g., H_2SO_4-$KMnO_4$, hydrazine) which are environmentally harmful and the production process is time-consuming [6]. Recently, electrochemical exfoliation of various carbon precursors, including graphite rods, carbon papers or HOPG, has been demonstrated to be an effective approach for generating graphene. Using

J. Liu, *Graphene-Based Composites for Electrochemical Energy Storage*,
Springer Theses, DOI 10.1007/978-981-10-3388-9_2

graphite rods as electrodes and ionic-liquid/water solution as electrolyte, Ionic liquid functionalized graphene sheets have been prepared *via* a one-step electrochemical approach [7]. Lu et al. [8] performed a detailed study and proposed a mechanism for the electrochemical exfoliation of graphite in ionic liquid solution, which involves (i) anodic oxidation of water, (ii) hydroxylation or oxidation of graphite edge planes, (iii) intercalation by ionic liquid anions between graphite layers, forming the graphite-intercalation-compounds (GICs), and (iv) oxidative cleavage and precipitation of the GICs. Inspired by the electrochemical reactions between graphite anode and organic carbonates in lithium ion batteries, Wang et al. [9] successfully prepared graphene flakes with few-layer *via* electrochemical exfoliation of graphite in propylene carbonate (electrolyte). The solvation nature of the bulky organic ions or molecules facilitate the intercalation process and the expansion of graphene layers. However, the organic compounds are sensitive to moisture and oxygen and the reactions always take a long reaction time. All these impede their practical applications. In the past few decades metal chlorides, strong protonic acids and other inorganic reagents have been the most promising "invaders" for graphite intercalation [10]. The expansion of graphite sheets in these intercalated compounds was realized by violent releasing of gases via fast heating. Very recently electric power has been used to drive the expansion and exfoliation of sulfate-intercalated graphite. In an electrochemical cell using protonic acid aqueous solution as electrolyte Su et al. [11] applied a relatively high (10 V) voltage to graphite anode for the synthesis of graphene sheets. Among many different electrolytes examined, including HBr, HCl, HNO_3, and H_2SO_4, only H_2SO_4 exhibits ideal exfoliation efficiency from natural graphite flake or highly oriented pyrolytic graphite. In Su's paper the anode (graphite) and cathode (Pt) were placed parallel with a separation of a few cm away. Similarly almost all the reported electrochemical cells for graphite exfoliation are in the parallel configuration.

Herein an improved synthesis of high-quality graphene is demonstrated in a vertical cell configuration *via* multiple electrochemical exfoliation of graphite rod [12]. Unlike previous reports, the unique cell configuration adopted here enables multiple exfoliation processes to improve both the quality and yield of graphene sheets. The mechanism of multiple electrochemical exfoliation of spent graphite rod was discussed in detail, the experiment conditions were optimized, and the structure and electrocatalytic activity of the resultant sample were investigated.

2.2 Experiment and Characterization

2.2.1 Material Synthesis

Synthesis of Graphene Flakes. Graphene flakes were prepared *via* multiple electrochemical exfoliation (MEE) approach. Briefly, graphite rod from spent Zinc-Carbon dry cells was utilized as positive electrode and the carbon source.

The anode (graphite rod) and cathode (platinum wire) were placed at the bottom and top of the electrochemical cell, respectively, with protonic acid (e.g. H_2SO_4, H_3PO_4 or $H_2C_2O_4$) aqueous solution as electrolyte. The electrochemical exfoliation process was ignited upon the application of a certain voltage across the electrodes. The water soluble graphene flakes were ultrasonicated, washed, dried and collected. Control experiments were also conducted *via* conventional (parallel) electrochemical configuration.

Synthesis of Nitrogen-doped Graphene Flakes. The as-prepared graphene flakes were annealed at 800 °C for 1 h under the flow of Ar/NH_3 (95/5, v/v, 400 sccm), to achieve the N-doped graphene.

2.2.2 Material Characterization

Structure and Morphology Characterization. The morphology was investigated *via* Scanning Electron Microscopy (SEM), Transmission Electron Microscopy (TEM, JEM-2010, 200 kV), Optical Microscopy and Atomic Force Microscopy (AFM, Nanoscope V, diDimension). Fourier transform infrared spectroscopy (FTIR) (Perkin Elmer 2000 FTIR spectrometer), Thermogravimetric Analysis (TGA) and X-ray photoelectron spectroscopy (XPS) [VG ESCALAB 250 spectrometer (Thermo Electron, Altrincham, U.K.), using an Al $K\propto$ X-ray source (1486 eV)] were used to shed more light on chemical composition information.

Electrochemical Performance Evaluation. Rotating disk electrode (RDE) and Cyclic voltammerty (CV) measurements were conducted in a standard three-electrode system (platinum foil-counter electrode, Ag/AgCl electrode-the reference electrode, Graphene-working electrode). The working electrode was prepared as follows [13]: (i) 10 mg of N-doped graphene was ultrasonically dispersed into1 ml of 2-propanl containing Nafion solution (5 wt%, dupont); (ii) 10 μl of the catalyst ink was coated on the glassy carbon disk (5 mm in diameter) and dried at 80 °C for 15 min. As-prepared graphene, pt-loaded carbon catalyst (Pt/C 20% on Vulcan XC-72R, E-TEK division, PeMEAS Fuel Cell Technology) with the same amount, and the bare glassy carbon electrode were tested for comparison. Methanol toxicity test was conducted at a constant potential −0.5 V (vs. Ag/AgCl). The voltammertic stability tests were performed in O_2-saturated 0.1 M KOH within the potential window of −1.0–0.2 V (vs. Ag/AgCl) for 20,000 cycles. The sweep rate is 100 mV/s. All measurements were carried out at room temperature. All potentials presented in the graphs and in the discussion were calibrated with reference to the reversible hydrogen electrode (RHE), which is independent of pH value. The number of electron transferred (n) was calculated based on Koutecky-Levich equation.

2.3 Results and Discussions

2.3.1 The Synthesis of Graphene Flakes

Different from conventional parallel two-electrode electrochemical cell, in our design graphite rod obtained from spent Zn–C primary battery (anode) and platinum wire (cathode) were placed vertically at the bottom and top of the electrochemical cell, respectively. The graphite rod was surrounded with a plastic tube and only the top surface of it was exposed to the electrolyte solution. A constant current of 0.1A was applied across the two electrodes. The potential of 6–8 V could drive the anions into the intercalation space and make the exfoliation to proceed. Comparative experiment was also conducted *via* conventional method. An apparent colour change for the aqueous electrolyte solution from transparent to dark was observed in vertical cell after only few minutes. This response time is much shorter than that of conventional method, indicating the exfoliation process in the vertical configuration is more efficient. In the same reaction time period, significantly larger quantity of graphene sheets were collected, benefiting from the multiple electrochemical exfoliation feature in our design. More details about the underlying mechanism will be discussed later.

The morphological and structural properties of the resultant samples were investigated by TEM, AFM and Optical microscopy. TEM and optical images reveal that the as-prepared products consist of a large amount of exfoliated graphene with lateral size ranging from 1 to few μm (Fig. 2.1a, c and d). The exfoliated graphene flakes with thickness of 4.84 nm are identified (Fig. 2.1b). Based on the statistical AFM mapping of exfoliated graphene flakes, approximately 32% of the graphene flakes have thicknesses in the range of 4–6 nm while nearly 80% of them are located in the thickness range of 4–8 nm (Fig. 2.1d). In addition, the total yield of graphene flakes is nearly ~50%, which is two folds of that of the control design.

FT-IR, XPS, and Thermogravimetric analysis (TGA) were employed to shed more light on the element information of the resultant samples. The presence of various functional groups including C–O (at 1060 cm^{-1}), C–O–C (1250 cm^{-1}), C=O/COO (at 1690–1710 cm^{-1}), and COO–H/CO–H (1365 cm^{-1}) [14] was observed (Fig. 2.2a). These functional groups can be eliminated by heating. The weight loss at ~100 °C in TGA (Fig. 2.2b) is due to the vaporization of adsorbed moisture or water. There is a major weight loss that starts at ~150 °C and continues up to 800 °C, which certainly results from the decomposition of functional groups. More significant loss for "MEE" graphene than "SEE" one (30% wt. vs. 20% wt.) indicates there are less functional groups on the "SEE" sample [15]. The presence of oxygen functional groups is further verified by XPS C1 s spectra

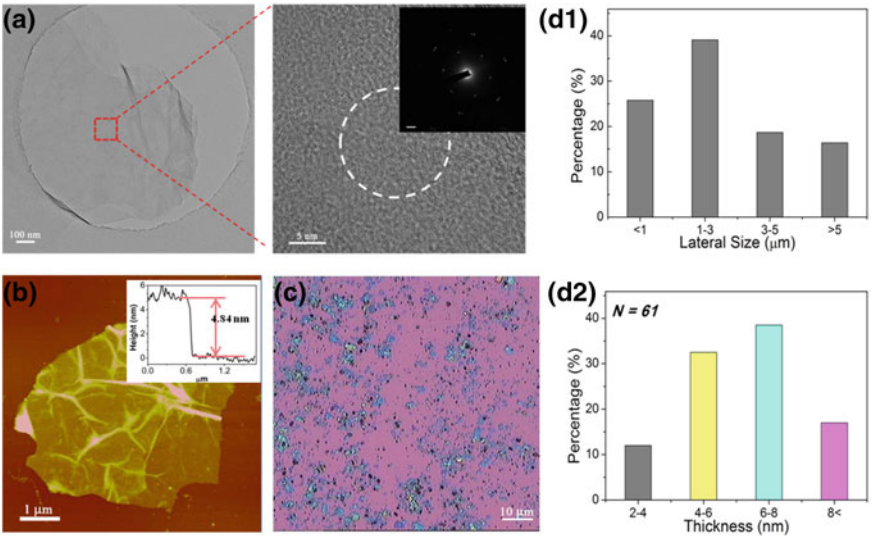

Fig. 2.1 **a** TEM image and corresponding selected area electron diffraction pattern of the multiple electrochemical exfoliation (MEE) graphene flakes. **b** AFM image of exfoliated graphene flakes spin-coated onto a SiO_2 (285 nm)/Si substrate. The thickness is ~4.84 nm, corresponding to 10–15 layers. **c** The low-magnification optical microscopy image of the MEE graphene flakes on SiO_2/Si substrate. **d** Lateral size and thickness distribution histograms of the MEE graphene sheets, as estimated from corresponding AFM images. The graphene flakes are mainly distributed in the range of 2–8 nm thickness (~80%) with lateral size about 1–5 μm. Figure reproduced from Ref. [12]

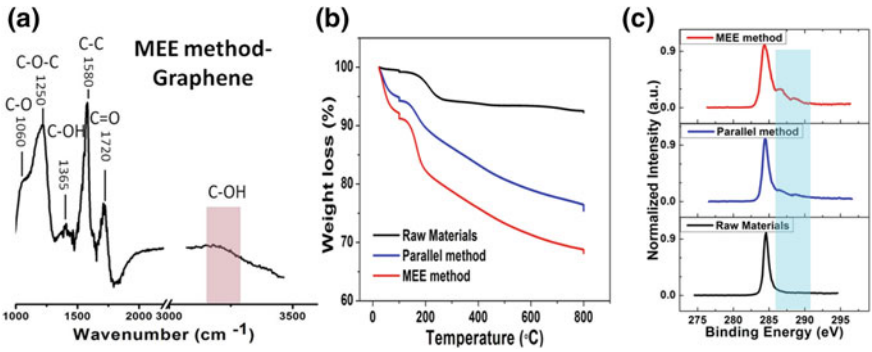

Fig. 2.2 **a** FTIR spectrum, **b** TGA plots and XPS C1 s spectra **c** for raw materials, parallel configuration graphene flakes and MEE graphene flakes

(Fig. 2.2c). In which, the peaks at 286, 287 and 289 eV in XPS C1 s spectra (blue area), which are assigned to C–O, C=O and carboxyl groups, respectively, were identified. This corroborates the significant oxidization of MEE graphene [16].

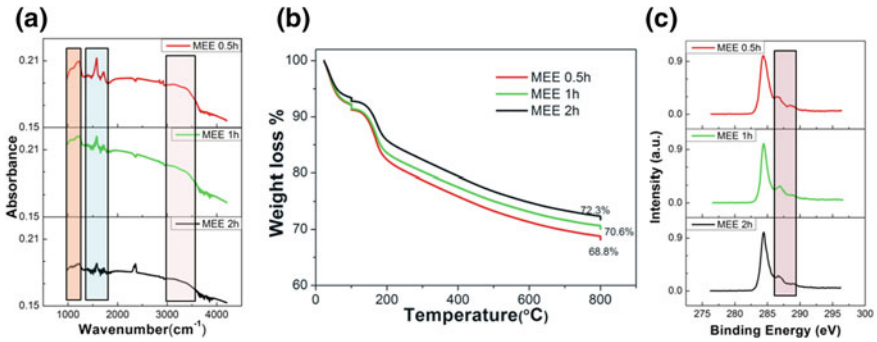

Fig. 2.3 FT-IR spectra **a**, TGA curves **b** and XPS C1 s spectra **c** of MEE GO prepared with different reaction time

The electrolysis time is found to be important for controlling the quality of graphene, including oxidization state, thickness/lateral size distribution and production efficiency. Specially, the FTIR intensity of typical functional groups peaks, such as C–O (at 1060 cm^{-1}) and C–O–C (1250 cm^{-1}), C=O stretch in carboxylic acid (1690–1710 cm^{-1}), and COO–H/CO–H (1365 cm^{-1}) remarkably decrease with the increase of exfoliation time (Fig. 2.3a). This is attributed to the remove of function groups upon heating with prolonging the reaction time [17]. This phenomenon is further confirmed by TGA results, in which slightly decrease in the total weight loss are observed (Fig. 2.3b), i.e. 31.2%, 29.4% and 27.7% for MEE 0.5 h, MEE 1 h and MEE 2 h, respectively. Particularly, a remarkable decrease in hydroxyl content (C–O, 286.6–286.8 eV) was observed from MEE 0.5 to MEE 2 h (Fig. 2.3c).

Electrolyte plays an important in efficient electrochemical exfoliation of graphene precursors. Various aqueous protonic acids including phosphoric acid, oxalic acid, sulfuric acid, acetic acid and formic acid were explored. These acids with bulky anions, such as phosphoric acid, sulfuric acid, and oxalic acid were proven to be effective in the exfoliation of spent graphite rod. The diverse choices of aqueous electrolyte provide us with more freedom to adjust the oxidization states of exfoliated graphene and reduce the production cost further. Oxalic acid solution is of particular interest due to: (i) the exfoliation process is faster; (ii) the oxalic acid exfoliated graphene exhibit better solubility in DI water, and (iii) the post-treatment is much easier. Poor performance have been observed for formic acid and acetic acid. This probably results from the weak anion salvation and weak expansion of graphite sheets upon the intercalation of HCOO– or H_3CCOO–, due to the their smaller size [18].

Previously reports indicated that the successful electrochemical exfoliation of graphite was strongly dependent on the graphite structure, and hence exfoliation

was observable only on high quality crystalline graphite such as HOPG, natural graphite flakes or paper [19, 20]. In our design, there is no special requirement on the quality and morphology of graphite source. Recycled graphite rod obtained from spent Zn–C primary batteries and pencil core could be equally well exfoliated without the need of special pre-treatment or cleaning. This design would no doubt pave the way for the commercialization of graphene, and also open up a wide opportunity for recycling of spent graphite in future.

2.3.2 *The Mechanism for Electrochemical Exfoliation*

Upon a high potential (~6–8 V) is applied across the two electrodes, the electrolyte anions such as OH^-, HSO_4^- and SO_4^{2-} and their solvated complexes (in the case of dilute H_2SO_4 being used as the electrolyte) are driven to graphite anode (Fig. 2.4). Electrochemical oxidation reactions (Eqs. 2.1–2.4) including the anodic

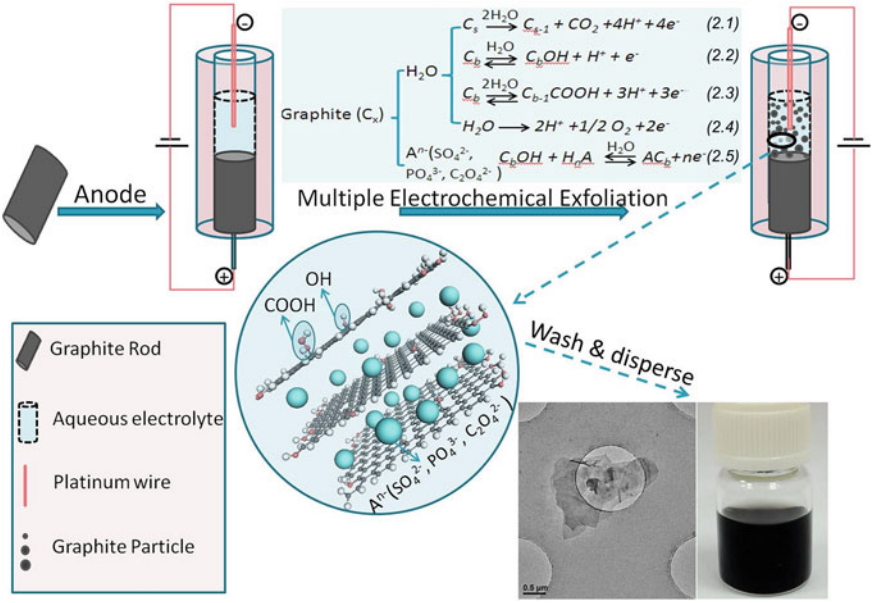

Fig. 2.4 Schematics of multiple electrochemical exfoliation (MEE) process. The digital photograph of the dispersed exfoliated graphene sheets in DMF solution, and the corresponding typical TEM images are shown. The mechanism of electrochemical exfoliation that consisting of anodic oxidation of graphite (Eqs. 2.1–2.3) and water (Eq. 2.4), and the intercalation of anions into graphite rod (C_s−surface of graphite rod, C_b−bulk of graphite rod) (Eq. 2.5), is illustrated. Schematic of graphite intercalation compound (GIC) with both hydroxyl and carboxyl groups formed is shown. Figure reproduced from Ref. [12]

oxidation, hydroxylation and carboxylation of graphite (as well as water oxidation), were triggered by the current flow accompanying with the remove of the electrons from anode (Fig. 2.4). These processes take place initially at the surface, grain boundary or structural defect sites, generating •OH, •COC, CO•, and COO• functional groups on the graphite surface. During these processes, CO_2 and O_2 can be produced as the electrolysis products (Eqs. 2.1 and 2.4) [21, 22]. The release of gaseous bubbles was obviously observed during the electrochemical process, which became vigorous with increasing exfoliation time, as if water boiled. The anodic corrosion/etching as well as the violent gas release open up the edge sheets of the graphite rod and facilitate the intercalation of bulky anions (as well as their solvated moieties) into the graphite layers, forming graphite-intercalation-compounds (GIC) ($C + A^- \rightarrow CA + e^-$) (Eq. 2.5). The intercalation and the hydrolysis of the intercalated complex ($CA + H_2O \rightarrow COH + H^+ + e^-$) [18, 23] lead to the expansion of graphene sheets and the cleavage/exfoliation of functional graphene sheets. Here, a mixture of GIC and graphite oxide is obtained. The exfoliated particles can be pushed up by the gas bubbles if they are small in size or light in weight. Or they would sink if the exfoliated particles are large and heavy. Nevertheless the precipitating big GIC particles can continue the electrochemical exfoliation when they have electric contact with anode. Multiple exfoliation process would proceed until smaller graphene sheets form and suspend in the solution. Therefore, the exfoliated graphene sheets produced in vertical design are thinner and better distributed in layer numbers.

2.3.3 *Electrochemical Performance of Resulted Graphene Flakes*

The graphene flakes were used as electrocatalysts for oxygen reduction reaction (ORR). To optimize their electrocatalytic performance further, nitrogen-doping was performed *via* annealing as-prepared MEE-Graphene in Ar/NH_3 atmosphere. The appearance of N1 s peaks and a sharp decrease in the intensity of O1 s peaks in XPS spectra corroborate the incorporation of N, and the reduction/remove of functional groups. The calculated N/C atomic ratio is 5.4 atomic %, similar to the values of N-doped graphene [24, 25]. The high resolution XPS N1s spectrum reveals the presence of pyridinic N (398.2 eV), pyrrolic N (400.5 eV), quantury N (401.1 eV) and N-oxides of pyridinc N (402.1 eV). These nitrogen-doped active sites are of particular interest for improving ORR electrocatalytic performance of carbon materials [24, 25].

The ORR catalytic activities of the MEE graphene before and after N-doped were investigated using rotating disk electrode (RDE) measurements in O_2−saturated 0.1 M KOH electrolyte (Fig. 2.5). A clear two-step process with

onset potentials at 0.82 V and 0.40 V, respectively, has been identified for the as-prepared MEE graphene, consisting well with previous reports on pure CNT [26] and graphene [27] (Fig. 2.5a). On the other hand the N-doped graphene electrode exhibits a well-defined, one-step process, suggesting a four-electron pathway for ORR on N-doped graphene (Fig. 2.5b). Furthermore, a much more positive ORR onset potential (0.92 V, *vs.* RHE) and higher cathodic currents are identified, corroborating the enhanced ORR catalytic performance [28]. The increase in electrocatalytic sites during N-doping process and the reduction of graphene are responsible for the enhanced ORR activities. Moreover, the corresponding Koutecky-Levich plots at different potential exhibit good linearity, and their slops were nearly the same over the potential range of 0.65–0.80 V, indicating the first-order reaction kinetics with almost constant electron-transfer numbers for ORR over a wide electrode potential (inset in Fig. 2.5b) [29]. The electron-transfer number n was calculated to be 3.9 according to the slopes of Koutecky-Levich plots, suggesting that nearly four-electron transfer process taken place in this potential range.

The stability tests were conducted in order to confirm the feasibility of MEE N-doped graphene for ORR application. There is only slightly decrease in limiting current, and the onset potential remains the same (Fig. 2.5c). The good catalytic stability was further confirmed by the overlap of CV curves before and after 20,000

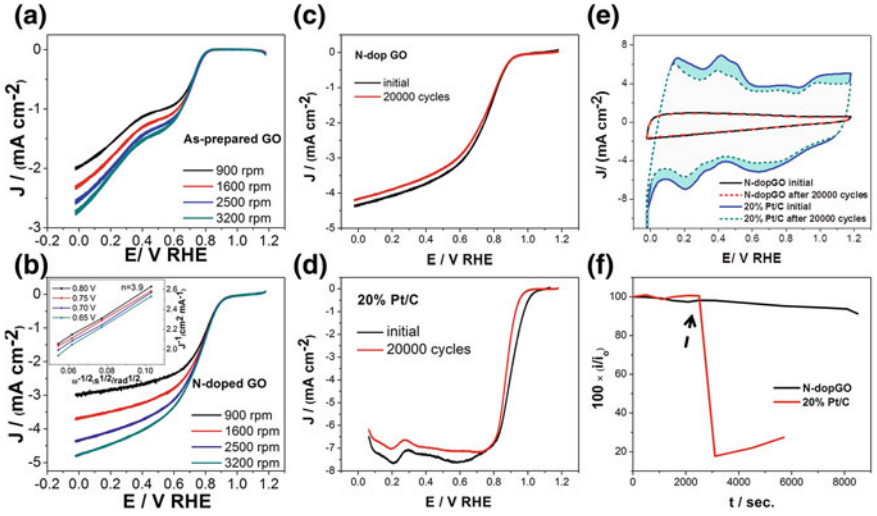

Fig. 2.5 ORR curves for as-prepared graphene **a** and N-doped graphene **b** in O_2−saturated 0.1 M KOH solution. The inset in **b** shows corresponding Koutecky-Levich plots derived from the ORR measurements. Polarization curves of N-doped G **c** and 20% Pt/C catalysts **d**, before and after 20,000 potential cycles. (Sweep rate, 100 mV/s; rotating rate, 2500 rpm.) **e** Cyclic Voltammerty curves of N-doped GO and 20% Pt/C catalysts before and after 20,000 cycles. **f** Current (i)-time (t) chronoamperometric responses to methanol. The arrow indicates the addition of 2% (weight ratio) methanol. Figure reproduced from Ref. [12]

cycling (Fig. 2.5e). Unlike N-doped graphene electrode, negative shifts in onset potential, reduction in limiting current as well as loss of surface area of CV curves were observed for 20% Pt/C electrode (Fig. 2.5d and e).

The N-doped graphene was further subjected to test the poisoning effect in the presence of methanol. As illustrated in Fig. 2.5f, the current response decreases sharply upon the addition of 2 wt% methanol for 20% Pt/C electrode. In contrast, the N-doped graphene electrode displays a strong and stable amperometric response, indicating a high selectivity due to the much lower ORR potential than that required for oxidization of methanol molecules [27, 30].

2.4 Conclusion

In conclusion, a simple, green and cost effective multiple electrochemical exfoliation approach has been proposed for synthesizing graphene in high quality and quantity. The mechanism of multiple electrochemical exfoliation of graphite was elucidated in detail. The experiment conditions are optimized. The nitrogen-doped graphene sheets have been demonstrated to deliver good electrocatalytic activity, stability and toxicity tolerance for alkaline electrolyte-based oxygen reduction reaction. Our present findings pave the way for scaled-up preparation, and further commercialization of graphene in a low cost and environmentally friendly way.

References

1. K.S. Novoselov, A.K. Geim, S.V. Morozov, D. Jiang, Y. Zhang, S.V. Dubonos, I.V. Grigorieva, A.A. Firsov, Electric field effect in atomically thin carbon films. Science **306**, 666–669 (2004)
2. S. Bae, H. Kim, Y. Lee, X.F. Xu, J.S. Park, Y. Zheng, J. Balakrishnan, T. Lei, H.R. Kim, Y.I. Song, Y.J. Kim, K.S. Kim, B. Ozyilmaz, J.H. Ahn, B.H. Hong, S. Iijima, Roll-to-roll production of 30-inch graphene films for transparent electrodes. Nat. Nanotechnol. **5**, 574–578 (2010)
3. X.S. Li, W.W. Cai, J.H. An, S. Kim, J. Nah, D.X. Yang, R. Piner, A. Velamakanni, I. Jung, E. Tutuc, S.K. Banerjee, L. Colombo, R.S. Ruoff, Large-area synthesis of high-quality and uniform graphene films on copper foils. Science **324**, 1312–1314 (2009)
4. K.V. Emtsev, A. Bostwick, K. Horn, J. Jobst, G.L. Kellogg, L. Ley, J.L. McChesney, T. Ohta, S.A. Reshanov, J. Rohrl, E. Rotenberg, A.K. Schmid, D. Waldmann, H.B. Weber, T. Seyller, Towards wafer-size graphene layers by atmospheric pressure graphitization of silicon carbide. Nat. Mater. **8**, 203–207 (2009)
5. S. Park, R.S. Ruoff, Chemical methods for the production of graphenes. Nat. Nanotechnol. **4**, 217–224 (2009)
6. X.L. Li, H.L. Wang, J.T. Robinson, H. Sanchez, G. Diankov, H.J. Dai, Simultaneous nitrogen doping and reduction of graphene oxide. J. Am. Chem. Soc. **131**, 15939–15944 (2009)
7. N. Liu, F. Luo, H.X. Wu, Y.H. Liu, C. Zhang, J. Chen, One-step ionic-liquid-assisted electrochemical synthesis of ionic-liquid-functionalized graphene sheets directly from graphite. Adv. Funct. Mater. **18**, 1518–1525 (2008)

8. J. Lu, J.X. Yang, J.Z. Wang, A.L. Lim, S. Wang, K.P. Loh, One-pot synthesis of fluorescent carbon nanoribbons, nanoparticles, and graphene by the exfoliation of graphite in ionic liquids. ACS Nano **3**, 2367–2375 (2009)
9. J.Z. Wang, K.K. Manga, Q.L. Bao, K.P. Loh, High-yield synthesis of few-layer graphene flakes through electrochemical expansion of graphite in propylene carbonate electrolyte. J. Am. Chem. Soc. **133**, 8888–8891 (2011)
10. O. Shornikova, N. Sorokina, N. Maksimova, V. Avdeev, Graphite intercalation in the graphite-H_2SO_4-R (R = H_2O, C_2H_5OH, C_2H_5COOH) systems. Inorg. Mater. **41**, 120–126 (2005)
11. C.Y. Su, A.Y. Lu, Y.P. Xu, F.R. Chen, A.N. Khlobystov, L.J. Li, High-quality thin graphene films from fast electrochemical exfoliation. ACS Nano **5**, 2332–2339 (2011)
12. J. Liu, C.K. Poh, D. Zhan, L. Lai, S.H. Lim, L. Wang, X. Liu, N. Gopal Sahoo, C. Li, Z. Shen, J. Lin, Improved synthesis of graphene flakes from the multiple electrochemical exfoliation of graphite rod. Nano Energy **2**, 377–386 (2013)
13. F.B. Su, Z.Q. Tian, C.K. Poh, Z. Wang, S.H. Lim, Z.L. Liu, J.Y. Lin, Pt Nanoparticles supported on nitrogen-doped porous carbon nanospheres as an electrocatalyst for fuel cells. Chem. Mater. **22**, 832–839 (2010)
14. Y. Si, E.T. Samulski, Synthesis of water soluble graphene. Nano Lett. **8**, 1679–1682 (2008)
15. D.C. Marcano, D.V. Kosynkin, J.M. Berlin, A. Sinitskii, Z.Z. Sun, A. Slesarev, L.B. Alemany, W. Lu, J.M. Tour, Improved synthesis of graphene oxide. ACS Nano **4**, 4806–4814 (2010)
16. D.V. Kosynkin, A.L. Higginbotham, A. Sinitskii, J.R. Lomeda, A. Dimiev, B.K. Price, J.M. Tour, Longitudinal unzipping of carbon nanotubes to form graphene nanoribbons. Nature **458**, 872–U875 (2009)
17. H.K. Jeong, Y.P. Lee, M.H. Jin, E.S. Kim, J.J. Bae, Y.H. Lee, Thermal stability of graphite oxide. Chem. Phys. Lett. **470**, 255–258 (2009)
18. M. Bottomley, A.R. Ubbelohde, G.S. Parry, D.A. Young, Electrochemical preparation of salts from well-oriented graphite. J. Chem. Soc. 5674–5680 (1963)
19. G.M. Morales, P. Schifani, G. Ellis, C. Ballesteros, G. Martinez, C. Barbero, H. J. Salavagione, High-quality few layer graphene produced by electrochemical intercalation and microwave-assisted expansion of graphite. Carbon **49**, 2809–2816 (2011)
20. D. Wei, L. Grande, V. Chundi, R. White, C. Bower, P. Andrew et al., Graphene from electrochemical exfoliation and its direct applications in enhanced energy storage devices. Chem. Commun. (2012)
21. F. Beck, H. Krohn, E. Zimmer, Corrosion of graphite-intercalation compounds. Electrochim. Acta **31**, 371–376 (1986)
22. F. Beck, H. Krohn, Reversible electrochemical intercalation of anions from aqueous-solutions in polymer bound graphite-electrodes. Synth. Met. **7**, 193–199 (1983)
23. F. Beck, H. Krohn, W. Kaiser, Galvanostatic cycling of graphite-intercalation electrodes with anions in aqueous acids. J. Appl. Electrochem. **12**, 505–515 (1982)
24. L.F. Lai, J.R. Potts, D. Zhan, L. Wang, C.K. Poh, C.H. Tang, H. Gong, Z.X. Shen, L.Y. Jianyi, R.S. Ruoff, Exploration of the active center structure of nitrogen-doped graphene-based catalysts for oxygen reduction reaction. Energy Environ. Sci. **5**, 7936–7942 (2012)
25. Z.Q. Luo, S.H. Lim, Z.Q. Tian, J.Z. Shang, L.F. Lai, B. MacDonald, C. Fu, Z.X. Shen, T. Yu, J.Y. Lin, Pyridinic N doped graphene: synthesis, electronic structure, and electrocatalytic property. J. Mater. Chem. **21**, 8038–8044 (2011)
26. K.P. Gong, F. Du, Z.H. Xia, M. Durstock, L.M. Dai, Nitrogen-doped carbon nanotube arrays with high electrocatalytic activity for oxygen reduction. Science **323**, 760–764 (2009)
27. L.T. Qu, Y. Liu, J.B. Baek, L.M. Dai, Nitrogen-doped graphene as efficient metal-free electrocatalyst for oxygen reduction in fuel cells. ACS Nano **4**, 1321–1326 (2010)

28. Y.Y. Liang, Y.G. Li, H.L. Wang, J.G. Zhou, J. Wang, T. Regier, H.J. Dai, Co(3)O(4) nanocrystals on graphene as a synergistic catalyst for oxygen reduction reaction. Nat. Mater. **10**, 780–786 (2011)
29. R.L. Liu, D.Q. Wu, X.L. Feng, K. Mullen, Nitrogen-doped ordered mesoporous graphitic arrays with high electrocatalytic activity for oxygen reduction. Angew. Chem.-Int. Edit. **49**, 2565–2569 (2010)
30. J. Liu, H. Yang, S.G. Zhen, C.K. Poh, A. Chaurasia, J. Luo, X. Wu, E.K.L. Yeow, N.G. Sahoo, J. Lin, Z. Shen, A green approach to the synthesis of high-quality graphene oxide flakes via electrochemical exfoliation of pencil core. RSC Adv. **3**, 11745–11750 (2013)

http://www.springer.com/978-981-10-3387-2

Graphene-based Composites for Electrochemical Energy Storage

Liu, J.

2017, XIII, 105 p. 39 illus., 34 illus. in color., Hardcover
ISBN: 978-981-10-3387-2